

Case Report

Human Midbrain Participates In Mismatch Detection Without Cognitive Activity Of The Cerebral Cortex: Case Report

Anna O. Kantserova^{1,2}, Lyubov B. Oknina¹, Eugeny L. Masherov³, Vitaly V. Podlepich³, Oleg S. Zaitsev³ and David I. Pitskhelauri³

¹Institute of Higher Nervous Activity and Neurophysiology of RAS, Moscow, Russia.

²Lomonosov Moscow State University, Moscow, Russia.

³N.N. Burdenko National Medical Research Center of Neurosurgery, Moscow, Russia.

***Corresponding Author:** Anna Kantserova, Institute of Higher Nervous Activity and Neurophysiology of RAS Butlerova str 5a, 117485, Moscow, Russian Federation, Lomonosov Moscow State University, Leninskie Gory GSP-1 119991, Moscow, Russian Federation, Tel: +79175178101; E-mail: anna.kantserova@gmail.com

Received: 02 August 2019; **Accepted:** 10 August 2019; **Published:** 12 August 2019

Abstract

Mismatch detection is the process of identification of rare stimuli from a sequence of stimuli. This important cognitive function is usually attributed to the cerebral cortex. To test the human midbrain involvement in sound mismatch detection, we recorded local field potentials in the states of deep anesthesia and clear consciousness from the drainage-electrode implanted in the cerebral aqueduct of an adult patient with an obstructive hydrocephaly who had undergone pineal region tumor removal through anterior interhemispheric transcalsal approach. We found a significant difference in the state of deep anesthesia at 256-364 ms after hearing a rarely presented sounds compared with frequently presented sounds and equally probable sounds. This difference was not found in the same experiment in the state of clear consciousness. The results suggest that human midbrain participates in mismatch detection and can do it even without cognitive activity of the cerebral cortex. Amplitude-frequency analysis of the midbrain records revealed that propofol affects the electrical activity of both human midbrain and cortex but the level of inhibition of the cortex is 6 times higher than the level of inhibition of the midbrain. We suppose that the human cortex is more susceptible to propofol than the human midbrain.

Keywords: Human midbrain; Deep electrodes; Deep anesthesia; ERP, Mismatch detection

Abbreviations

Amplitude-frequency (A-F)

Cerebrospinal Fluid (CSF)
Computed Tomography (CT)
Event-Related Potential (ERP)
Gamma-Aminobutyric Acid (GABA)
Inferior Colliculi (IC)
Local Field Potentials (LFP)
Periaqueductal Grey Substance (PAG)
Positron Emission Tomography (PET)
Signal-Space Projection (SSP)
Stimulus-Specific Adaptation (SSA)

Introduction

Today it is clear that the cortex is responsible for the basic cognitive functions in humans. However, the existence of some “primitive intelligence” like novelty detection in animals without cerebral cortex [7] and human mismatch negativity in sleep and anesthesia [17] led scientists to new research in this field. On the one hand, the human EEG research showed mismatch in the middle latency response (12–50 ms from sound onset) of auditory evoked potential [28]. On the other hand, the studies on the neurons of the laboratory animals inferior colliculi (IC) suggest that local mechanisms exist in the IC for suppressing neural responses to frequently presented sounds and enhancing responses to rarely presented sounds [3, 10,19,21,40,52,54]. Several studies claimed the novelty detection in the human auditory brainstem and in particular from IC [11,28,65,66], but there is still no direct electrophysiological evidence from the human midbrain.

Brainstem is “hidden” from scalp registration of electrophysiological activity. Therefore, it is very difficult to assess the mesencephalon cognitive activity. The registration of local field potentials (LFP) from deep structures has opened a new window towards the understanding of neural functions of the human midbrain. LFPs represent the aggregate activity of small populations of neurons represented by their extracellular potentials. One of the few articles, dedicated to LFPs from macroelectrodes implanted in periaqueductal grey substance (PAG), suggests that human infant vocalizations are subject to differential processing early in time in the human midbrain in consciousness [50]. This may represent an important first stage in the processing route that facilitates quick reactions to these biologically salient vocalizations.

The present study is aimed to investigate the electrical activity of the midbrain comparing with the cortex during deep propofol anesthesia and clear consciousness, to reveal the functional connectivity between the cortex and auditory brainstem and to explore the involvement of the human midbrain in mismatch detection.

The practical significance of the electrophysiological study of the human auditory midbrain lies in auditory midbrain implants [23,63]. Auditory brainstem implant (ABI) is an electronic device indicated for use when anatomic or functional characteristics do not allow to use of cochlear implant or other hearing technologies, such as fully implantable hearing aids and hearing aids for sound amplification. This is usually the case for individuals with Neurofibromatosis type 2, malformation or agenesis of cochlear nerves and/or cochlea, as well as in cases of cochlea ossification following meningitis

[5,39]. ABI allow hearing speech and environmental sounds. Results of speech perception vary widely - some studies have only reported increased attention to sound [8,48], while others have shown that ABI users presented sentence recognition results in open context in silence of 10% to 100% [16,23,27]. Nevertheless, further investigation is required for effective ABI placement [46]. Avoiding mismatch detection midbrain areas damage during ABI installation can benefit patients.

Materials And Methods

Patient

Ethical approval of the research methods was obtained from Burdenko Neurosurgery Center Research Ethics Committee. Participation of the patient in study was voluntary and the patient gave the written informed consent to take part in the study. The study included one male patient of 37 years old with tumor of the pineal region with obstructive hydrocephaly who underwent tumor removal through anterior interhemispheric transcallosal approach. Tumor was totally excised and aqueduct was widely opened. After removal of the tumor at the final stage of the operation, a specially developed external ventricular drainage was installed for 24 hours for the purpose of draining cerebrospinal fluid (CSF) and preventing possible CSF circulation disorders. Previous study showed the possibility of reliable intraoperative third ventriculostomy and aqueductal lifelong stenting in cases of surgical treatment of midline deep-seated brain tumors [56]. More information about the operation technique is available in the study [47].

Three ring electrodes (the two distal electrodes were recording and the proximal one was indifferent) 3 mm long were attached to the distal end of the drainage 3 mm (between recording electrodes) and 10 mm (between the deepest recording electrode and indifferent electrode) apart (Figure 1). Bipolar montage with distance between electrodes up to 5 mm allows to record LFP. In our study the distance between electrodes was 6.5 mm, but recorded event-related potentials (ERPs) still represented oscillations from brain structures which are close to the recording electrode. Deep electrodes (D1 and D2) positions were controlled by computer tomography (CT) (Figure1). Cortex potentials were recorded from 19 scalp electrodes located by the 10-20% system (FP1, FP2, F3, F4, F7, F8, Fz, C3, C4, Cz, P3, P4, Pz, T3, T4, T5, T6, O1, O2) using ear indifferent electrodes.

Brain potentials recording

The scalp and midbrain potentials were recorded simultaneously with Neurobotics system (Russia) using notch (50 Hz), high-pass (0.5 Hz) and low-pass (70 Hz) real time filters for online data quality evaluation.

CT was performed during transferring the patient to the intensive care unit after surgery. Aims of CT were verification of the ventricular drainage position and control of postoperative complications. During patient transportation and tomography, continuous propofol (6 mg/kg/hour) administration was performed for the purpose of patient sedation. The scalp and midbrain potentials recording was carried out immediately after patient admission to the intensive care unit. Then the whole complex of intensive care procedures was carried out and vital functions were monitored. The state of consciousness during these procedures is hereinafter referred to as deep anesthesia. No single stimulus or response to it exists that can measure the depth of anesthesia in a clinically or scientifically meaningful way [41]. After performing all the

manipulations and monitoring stabilization, the introduction of propofol was discontinued. Then the dexmedetomidine sedation was carried out to prevent hemodynamic reactions and excite the patient. The starting dose of dexmedetomidine was 1.4 µg/kg/hour. Further, the dose was gradually reduced (every 15 minutes by 25% of the initial dose) until full awakening and extubation. Patient's consciousness recovery was evaluated at each step of the sedation by the neuropsychiatrist.

Various auditory stimuli were presented to the patient during brain potentials recording in order to get event-related potentials (ERP). There were two experimental blocks of a 100 stimuli. The first was equiprobability paradigm: 600, 800, 1000 and 2000 Hz tones of a 25 stimuli each. In the state of deep anesthesia record lasted about 3 minutes. The second was two-tone oddball paradigm: 20 tones of 600 Hz and 80 tones of 800 Hz [57]. The volume of all sounds was 76 dB. In the state of deep anesthesia record lasted about 2 minutes. ERPs were recorded without any instruction (in passive conditions). The auditory stimuli intensity and the rate of stimulus presentation remained constant throughout the study.

Data analysis

Brain activity was analyzed with MATLAB (R2015b, Math Works, USA) Brainstorm toolbox. Statistical analysis was performed with STATISTIKA10 software. Band-pass filter (0.5-49 Hz) was initially applied to all records. Heartbeats were removed from deep anesthesia records with signal-space projection (SSP) approach. Bad channels were also removed from the records: T3 and T5 from deep anesthesia records, F7 and F8 from clear consciousness records. Brain activity records were subject to visual and amplitude-frequency analysis. Burst suppression ratio was counted for deep anesthesia records. The burst suppression ratio is a number between 0 and 1 which measures the fraction of time in a given time interval that the electroencephalogram is suppressed [59,60,61].

For amplitude-frequency (A-F) analysis, each record was cut into sections of two seconds. No artifact sections were selected. Then A-F spectra of all sections were put together in order to get amplitude distributions for each frequency. The resulting amplitude distributions for each frequency turned out to be abnormal (p -value $<0,05$ of Kolmogorov-Smirnov, Lilliefors and Shapiro-Wilk's test for normality). Hence we used medians for plotting. Similarity of cortex and midbrain A-F spectra was estimated with Mann-Whitney U test.

Quality of recording sites containing auditory stimuli was visually evaluated. Artifact sections were excluded from the study. Responses for each type of stimuli were averaged separately. The time domain of ERP included 100 ms of a pre-stimulus signal (baseline) and 500 ms of a post-stimulus signal. Additionally, 20 random recording sections were averaged in order to evaluate the noise level of ERP signal. Amplitudes and latencies of N60, P80, N120, P150 peaks of deep anesthesia were evaluated. Similarity of midbrain ERPs in the state of deep anesthesia was estimated with Mann-Whitney U test.

Functional connectivity of the brain signals between all pairs of electrodes was estimated using Bivariate Granger causality [47]. The value of model order $n=10$ (not greater than 5 frequency peaks in the spectrum assumed). It is widespread and used in the Brainstorm toolbox as default. Granger causality charts were visually analyzed for density and predominant

direction of links.

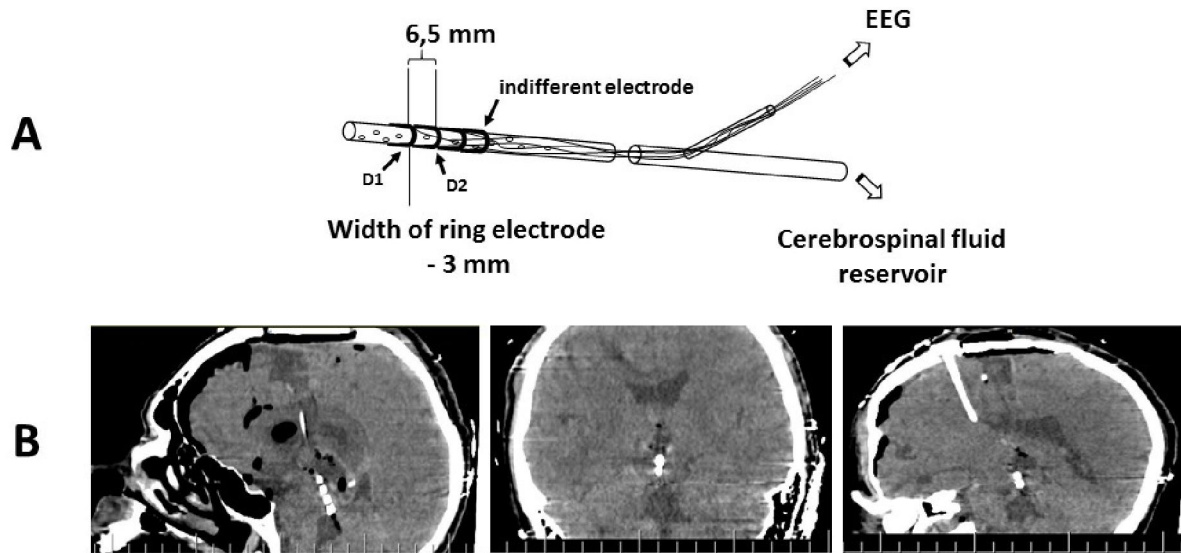


Figure 1: A – Schematic presentation of drainage-electrode. B – Postoperative CT scans demonstrating correct position of the drainage-electrode in the cerebral aqueduct.

Results

Amplitude-frequency spectra

In the state of deep anesthesia, the cortex activity was divided into bursts and suppressions (Figure 2). The bursts were rare and mostly consisted of alpha rhythm (12 Hz). The suppressions covered larger part of the recordings of cortex activity and had lower amplitude than alpha rhythm of bursts. Burst suppression ratio was approximately 0.92. In clear consciousness, records were monotonous.

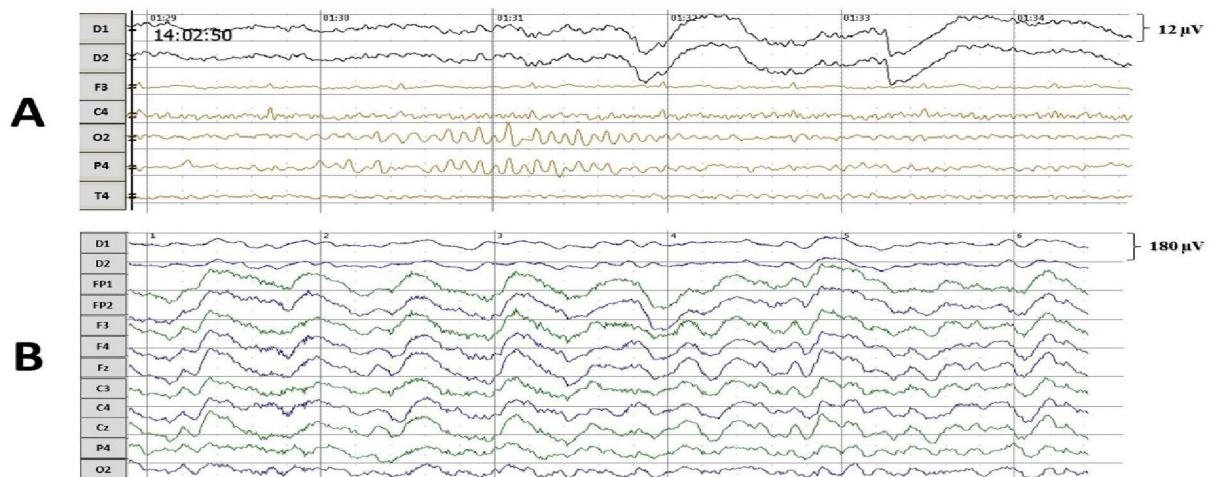


Figure 2: EEG from the midbrain (D1 and D2) and the scalp (other sites). A – the state of deep anesthesia (propofol 6 mg/kg/hour), scale 12 μV/sec. B – the state of clear consciousness, scale 180 μV/sec.

In the state of deep anesthesia, the activity recorded from scalp electrodes was lower amplitude comparing with deep electrodes and there were no dominant frequencies (peaks on the spektrum) (Figure 3). The greatest amplitude of brain activity in the clear consciousness was observed in the theta frequency range (5-8 Hz). Furthermore, the shape of amplitude-frequency spectrum of cortex activity was quite similar to shape of midbrain's amplitude-frequency spectrum in theta frequency range in consciousness (3-6 Hz).

The activity of the cortex changed most radically from deep anesthesia to clear consciousness (Figure 3). Its average amplitude increased by 29 times while the midbrain's average amplitude increased only by 5 times.

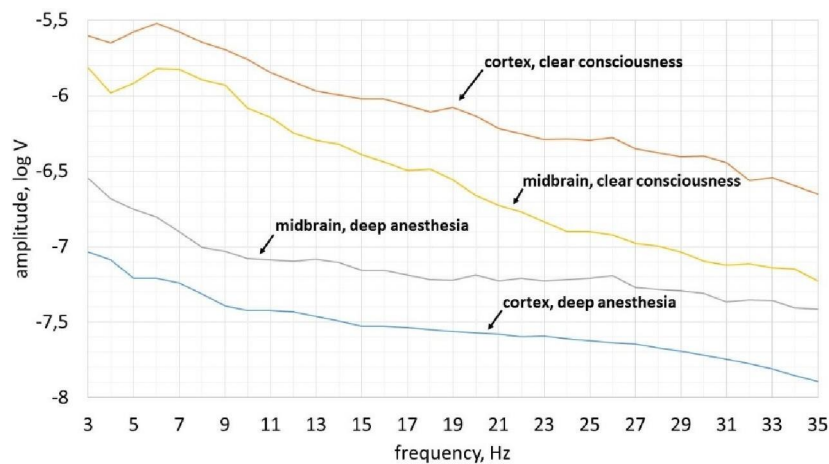


Figure 3: Amplitude-frequency spectra of cortex and midbrain activity in the state of deep anesthesia (dose of propofol 6 mg/kg/hour) and clear consciousness.

ERP and Granger causality

In the state of deep anesthesia, amplitude and shape of cortex ERP were close to noise or even below noise level (Figure 4). There were no peaks observed. But ERP from deep electrodes had very different shape and a lot of easily detected peaks (Figure 4). Midbrain ERP included onset of the tone part (peaks N60 and P80) and part specific to the frequency of the tone (latency around 100-200 ms). Peaks N60 and P80 had the similar latency at all ERPs in anesthesia (Table 1). The latencies of frequency-specific part were similar at 800 Hz and 600 Hz in both paradigms: oddball and equiprobability (Figure 4). On the contrary, the difference in amplitudes of N120 and P150 peaks was larger in oddball paradigm (Table 1). This difference was 3 times larger in response to rare tone of oddball paradigm than to equiprobability tone of 600 Hz and 1,2 times larger in response to frequent tone of oddball paradigm than to equiprobability tone of 800 Hz. Also in equiprobability paradigm, the difference in amplitudes of N120 and P150 peaks was larger in responses to low sounds (600 and 800 Hz) than high sounds (1000 and 2000 Hz). In addition, the response to the rare tone of oddball paradigm included a unique peak with latency 256-364 ms.

In clear consciousness, cortex ERPs were more monotonous and more traditional (Figure 4). There were only N100 peak

clearly detected in scalp ERP in response to 1000 and 2000 Hz and P300 peak in response to rare tones. The largest P300 response was observed on FP1 and FP2 scalp sites. Midbrain ERPs showed greater amplitude than those in the state of deep anesthesia were (Figure 5). There was no rare tone unique peak but frequency-specific peaks remained predominantly in response to 600 Hz and frequent tone (Figure 5 C and D).

Mann-Whitney U-test with ERP from D1 and D2 electrodes showed the insignificant difference between signals from these electrodes (Table 1). In addition, p-value in clear consciousness was higher than in the state of deep anesthesia.

paradigm	probability of tone's occurrence	frequency of the tone	latency of N60, ms	amplitude of N60, μ V	latency of P80, ms	amplitude of P80, μ V	Δ of amplitudes, μ V	latency of N120, ms	amplitude of N120, μ V	latency of P150, ms	amplitude of P150, μ V	Δ of amplitudes, μ V	p-value, propofol 5 ml	p-value, clear consciousness
oddball	20%	600 Hz	62	0,0487	78	0,6808	0,6320	112	0,1814	136	1,1354	0,9540	0,5780	0,9561
equiprobability	25%	600 Hz	64	0,6333	82	1,6551	1,0218	106	0,0419	134	0,3881	0,3462	0,5102	0,9658
oddball	80%	800 Hz	60	-0,5401	82	0,0665	0,6066	144	-1,2089	162	0,8634	2,0724	0,5575	0,9486
equiprobability	25%	800 Hz	60	-0,6976	80	0,6725	1,3701	140	-1,4009	158	0,3051	1,7060	0,5255	0,9371
equiprobability	25%	1000 Hz	60	-0,5051	80	0,3138	0,8189	142	-0,2691	168	0,2599	0,5290	0,9922	0,9103
equiprobability	25%	2000 Hz	60	-0,6793	78	0,0126	0,6919	136	0,4955	154	0,5977	0,1022	0,8846	0,9526

Table 1: Characteristic of ERP in the state of deep anesthesia

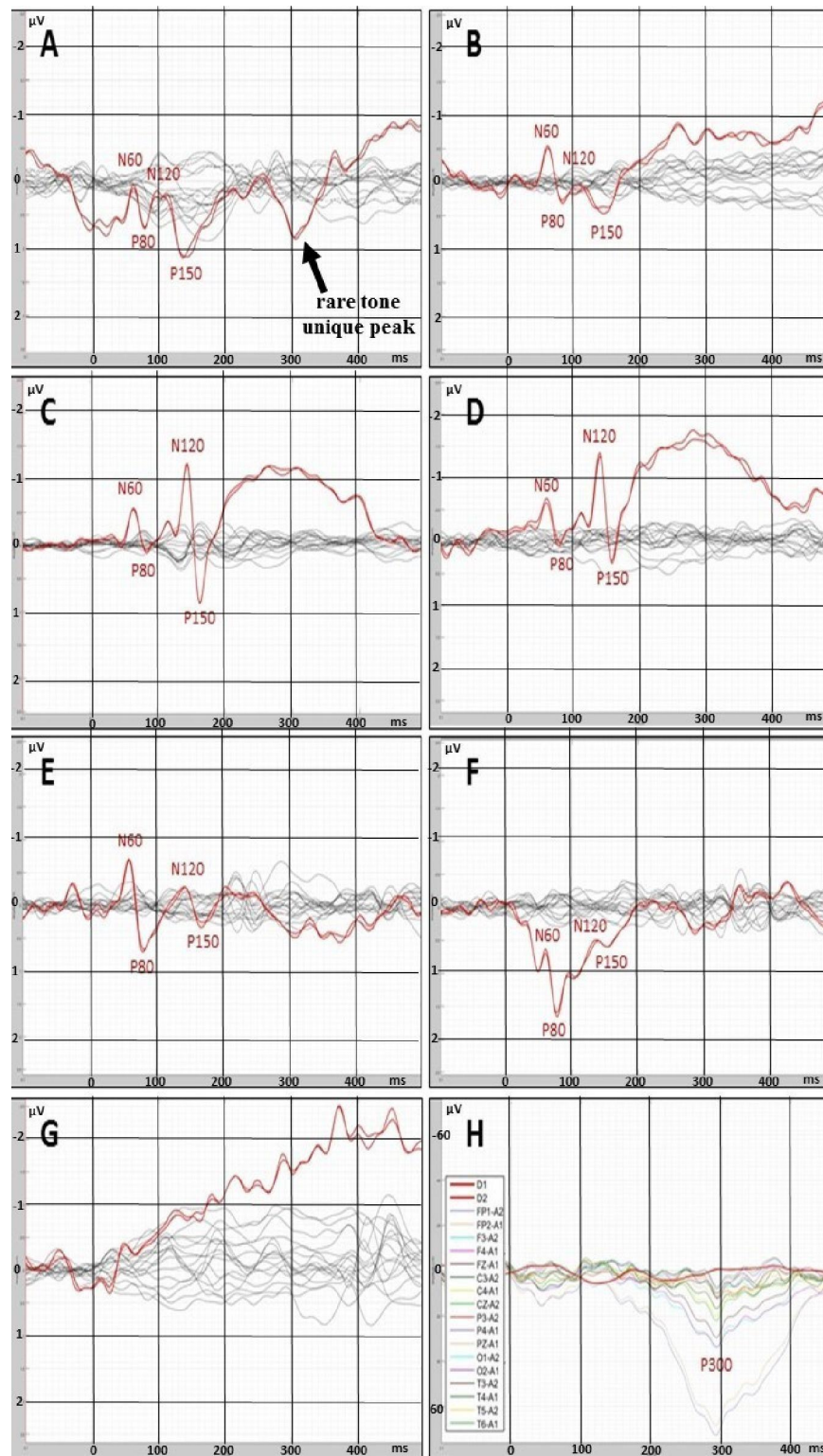


Figure 4: ERPs recorded with deep (red lines) and scalp (black or multicolor lines) electrodes. A – rare tone (oddball paradigm) in the state of deep anesthesia. B – tone of 600 Hz (equiprobability paradigm) in the state of deep anesthesia. C – frequent tone (oddball paradigm) in the state of deep anesthesia. D - tone of 800 Hz (equiprobability paradigm) in the

state of deep anesthesia. E - tone of 1000 Hz (equiprobability paradigm) in the state of deep anesthesia. F - tone of 2000 Hz (equiprobability paradigm) in the state of deep anesthesia. G - noise in the state of deep anesthesia. H – rare tone (oddball paradigm) in clear consciousness.

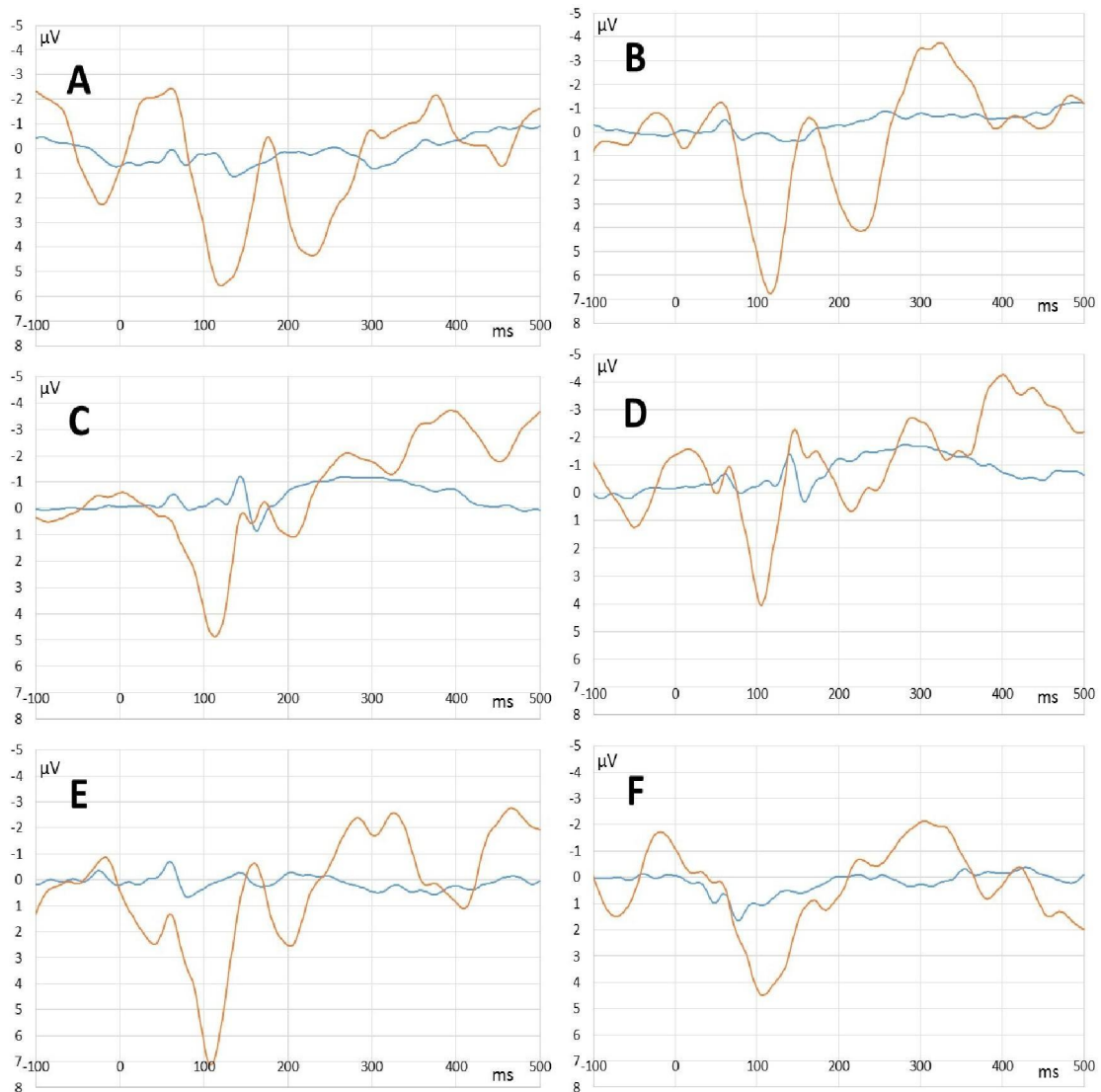


Figure 5: Midbrain ERPs recorded in the state of deep anesthesia (blue lines) and clear consciousness (orange lines). A – rare tone (oddball paradigm). B – tone of 600 Hz (equiprobability paradigm). C – frequent tone (oddball paradigm). D - tone of 800 Hz (equiprobability paradigm). E - tone of 1000 Hz (equiprobability paradigm). F - tone of 2000 Hz (equiprobability paradigm).

In the state of deep anesthesia, Granger causality showed the predominant number of connections from the midbrain to the cortex sites compared with number of connections from the cortex to the midbrain at the latency of rare-tone special peak (256-364 ms). The number of cortex-to-cortex connections was close to equiprobability tone of 600 Hz and the noise level (Figure 6).

In clear consciousness, Granger causality showed large number of connections from the frontal sites to other cortex sites compared to noise level at the latency of cortex P300 peak (200-400 ms). The midbrain sites were connected with each other from lower sensor (D1) to upper sensor (D2). The number of cortex-to-cortex connections in the responses to rare tone and equiprobability tone of 800 Hz was higher compared to noise level (Figure 6).

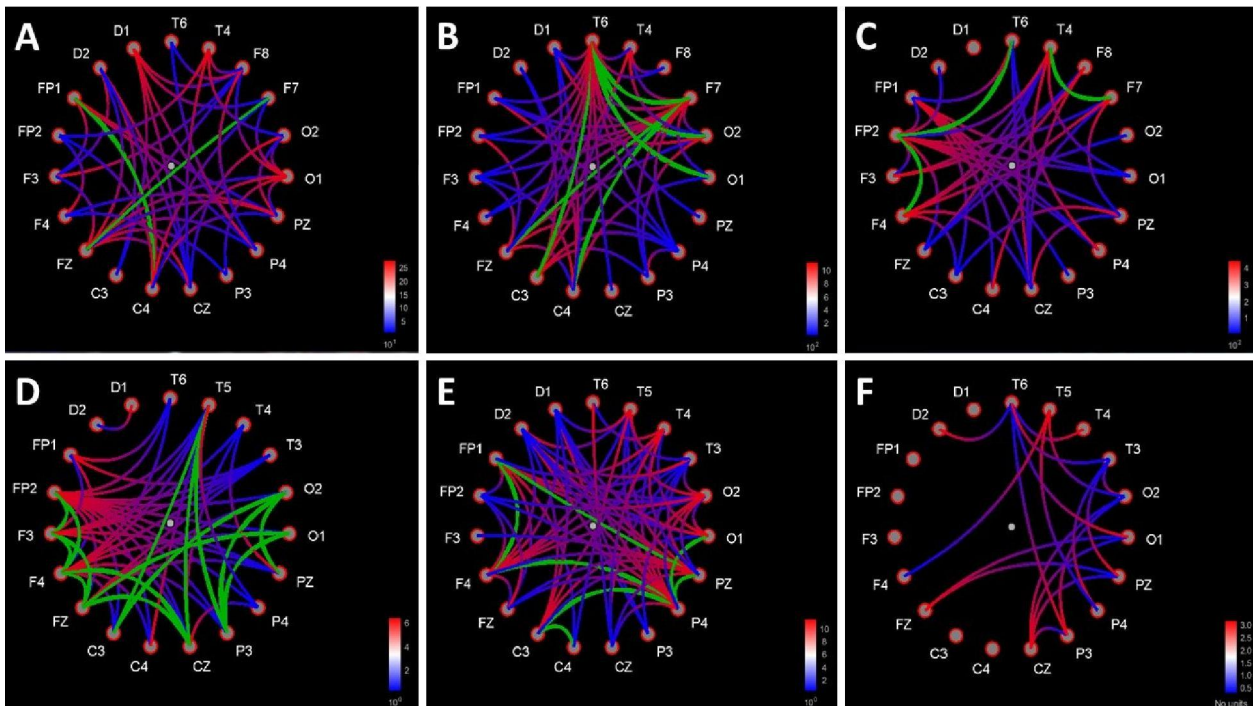


Figure 6: Functional connections between all pairs of sites charts based on Bivariate Granger causality method. Causality direction – from red to blue color of lines. Bi-directional links are marked with green color of lines. Distance filtering 0 mm. A - rare tone (oddball paradigm) in the state of deep anesthesia (the latency of rare tone special peak 256-364 ms, intensity trash 101-102). B - tone of 600 Hz (equiprobability paradigm) in the state of deep anesthesia (the latency of rare tone special peak 256-364 ms, intensity trash 101-102). C – noise in the state of deep anesthesia (the latency of rare tone special peak 256-364 ms, intensity trash 101-102). D - rare tone (oddball paradigm) in clear consciousness (the latency of P300 cortex peak 200-400 ms, intensity trash 1,91-1,95). E - tone of 600 Hz (equiprobability paradigm) in clear consciousness (the latency of P300 cortex peak 200-400 ms, intensity trash 1,91-1,95). F - noise in clear consciousness (the latency of P300 cortex peak 200-400 ms, intensity trash 1,91-1,95).

Discussion

Limitations of the experimental methods

There was no possibility to check the results in healthy subjects. So in this case report we investigated individual data instead of comparing with the control group. The published articles about healthy human auditory midbrain functioning in propofol-induced loss of consciousness are represented by contradictory positron emission tomography (PET) studies [25,33].

Deep electrodes were located in close proximity to the midbrain tissue. Scalp electrodes, on the other hand, received a

signal from the cortex through many layers of other tissues (skull bones, skin, etc.). Also deep and scalp electrodes had different reference electrodes. For these reasons, we decided not to compare the absolute values of the midbrain amplitudes and values of the cortex amplitudes signals but to focus on amplitude dynamics difference.

The CT scan resolution does not allow us to determine the exact positions of the deep electrodes relative to the structures of the midbrain. We can only claim that recorded deep electrodes were in the aqueductus cerebri near the border with the fourth ventricle. Therefore, the nature of electrophysiological signal from deep electrodes can be established by ERP analysis.

The total duration of records in the state of deep anesthesia did not exceed 10 minutes. This allows us to assume that the EEG in the state of deep anesthesia was recorded in the steady state of the brain. Contribution of consciousness recovery in the obtained data was not significant.

Propofol anesthesia features

Propofol, the most widely administered anesthetic agent, is used as an induction agent for sedation and maintenance of general anesthesia [55]. Propofol binds post-synaptically to gamma-aminobutyric acid (GABA) type A receptors where it induces an inward chloride current, which hyperpolarizes the post-synaptic neurons thus leading to inhibition [4,25]. In the cortex, propofol induces inhibition by enhancing GABA-mediated inhibition of pyramidal neurons [4]. Propofol decreases excitatory inputs from the thalamus to the cortex by enhancing GABAergic inhibition at the thalamic reticular nucleus, a network that provides important inhibitory control of thalamic output to the cortex [59]. Propofol also enhances inhibition in the midbrain at the GABAergic projections from the pre-optic area of the hypothalamus to the brainstem arousal centers: pedunculopontine tegmental, nucleus and the lateral dorsal tegmental nucleus, the locus ceruleus, the dorsal raphe nucleus and ventral periaqueductal grey substance [9]. The target areas of the dorsal raphe nucleus include the entire cerebral cortex, thalamus, hippocampus, amygdala, cerebellum, and numerous brainstem nuclei [69]. There are direct noradrenergic projections from the locus coeruleus to most of the cortical mantle [43,51]. The cholinergic nuclei which include the laterodorsal tegmental nucleus and the cholinergic portion of the pedunculopontine tegmental nucleus project to several thalamic nuclei including the reticular nucleus of the thalamus [49,67], and to basal forebrain regions such as the substantia innominata [44]. When delivered in a sufficiently high dose, i.e. deep anesthesia, propofol induces burst suppression in cortex EEG [1,15].

Amplitude-frequency analysis

The difference in amplitude of the IC electrical activity between consciousness and anesthesia was less than the difference in amplitude of the cortex electrical activity nearly by 6 times. It means that the human cortex is more susceptible to propofol than the midbrain. This fact can be explained by the direct effect of propofol on the cortical pyramidal neurons and the anatomical connections of the propofol target subcortical structures [59]. The predominant number of these connections are ascending and activating so their inhibition automatically reduces activity of the cortex. Therefore, midbrain receives less top-down signals from the cortex and is not excited by midbrain reticular formation neuronal

collaterals.

The greatest amplitude of cortex and midbrain activity in consciousness was observed in the theta frequency range (5-8 Hz). An increase in theta amplitude is common for the scalp EEG in case of brain lesions and correlates with the volume of the edema [24].

The similarity of the shapes of amplitude-frequency spectra from the deep and scalp electrodes is highest in the theta frequency range (3-6 Hz) too. The medial septum and diagonal band of Broca area are assumed to be the pacemaker of theta rhythm [30,35,36,38,68]. The predominant number of hypothesis of genesis of alpha rhythm based on thalamocortical system [2] or cerebral cortex only [37]. Beta activity is associated with motor and premotor cortex, the basal ganglia, the cerebellum [22]. So all the sources of alpha and beta activity are far from the deep electrodes and above it. Their signals must be filtered using depth reference electrode. On the contrary, the medial septum and diagonal band of Broca area are away from the brainstem axis. Thus, the signal from this source reached both deep and scalp electrodes equally well.

ERPs

N100 and P300 reflect the presence of cognitive processes (orienting processes, attention and stimulus classification) in the cortex in clear consciousness [18,45,70]. On the contrary, the absence of cortex ERPs in the state of deep anesthesia indicates cognitive inactivity of the cortex.

The fact of ERPs presence in midbrain and absence in the cortex also points to higher resistance of the midbrain structures to the propofol anesthesia.

Unexpectedly, midbrain ERPs clearly appeared in the state of deep anesthesia on the time interval 50-400 ms. Scalp recorded (vertex-mastoid) brainstem potentials usually situate in the first 8-15 ms of ERP and have a different shape [6,31,55]. Some papers revealed the invariability of the brainstem components of ERP in anesthesia with standard concentrations of propofol [64,71]. On the contrary, the predominant number of publications show dose dependent increase in the latencies of the brainstem auditory evoked response during propofol anesthesia [13,14,58]. The large increase in ERPs latencies confirms the effect of propofol on the midbrain activity. On the other hand, the presence of some frequency-specific peaks (50-200 ms) in midbrain ERPs in the state of clear consciousness was due to slowing the activity of the auditory brainstem structures because of the edema after surgery.

Unfortunately, there is no propofol bolus (deep propofol anesthesia) ERP data in literature.

According to the recent research, there is also a top-down influence of the cortex on the midbrain in the unanaesthetized brain, which is called meta-adaptation [62]. Meta-adaptation is the rapid adaptation of the auditory midbrain to complex sound environment. It decreases with inactivation of the auditory cortex. An absence of meta-adaptation could also contribute to increase of brainstem latencies.

The similarity of midbrain ERPs points to the location of the generating structures between two deep electrodes. It means that the structures are up to 6 mm long. The frequency-specific part indicates that this structure belongs to the auditory system. Based on these facts, we suppose that the recorded deep ERPs had inferior colliculus (IC) origin [34].

The values of amplitudes of frequency-specific parts of deep ERPs in equiprobability paradigm are consistent with experiments on awake monkey neurons [10]. In that study, the prevalence of low frequency (<2000 Hz) tuning neurons in IC was found. In our study the response to low tones was stronger comparing with high tones. There was also information about neurons on the periphery of the responsive area, which showed little or no tuning to tone frequency. The existence of such cells in IC may be important for rare tone unique peak generation.

The most unexpected was a rare tone unique peak with latency 256-364 ms. Several studies claimed the novelty detection in the human auditory brainstem and in particular from IC [11,28,65,66], but there is still no direct electrophysiological evidence from the exact structure of the human midbrain. However, in electrophysiological mammalian experiments a stimulus-specific adaptation (SSA) was shown in IC [19,21,40,54]. SSA is a form of short-term plasticity, a reduction in neural response to a repeated sound. Neurons with rapid and obvious SSA do not respond to repeating sound but recover their excitability very fast when frequency of the tone is changed [21]. SSA takes place in neurons of IC and serves as a basis for detection of novel sounds. A rare tone unique peak could be generated by IC cells that show little or no tuning to tone frequency [10].

However, fuzzy outlines of rare tone unique peak could be seen at 2000 Hz midbrain ERPs of equiprobability paradigm. This fact can be explained by higher subjective loudness of 2000 Hz tone comparing with 600, 800 and 1000 Hz with the same sound pressure level due to the features of transmission through the middle ear [26,42]. For this reason, the 2000 Hz tones could be deviant in volume in the paradigm of equally probable frequencies.

Moreover, the higher difference in amplitudes of N120 and P150 peaks in oddball paradigm showed the activation of more IC frequency tuning neurons in response to a more difficult task (especially in response to rarely presented sounds).

However, the presence of midbrain ERP peaks during deep anesthesia remains unclear. Propofol binds post-synaptically to GABA_A receptors and enhances GABA-mediated inhibition [4,29]. Several studies have thoroughly unraveled the role of GABAergic inhibition in subcortical mismatch detection using the microiontophoresis technique [12]. Subcortical mismatch detection is modulated by a gain-control mechanism mediated by GABA_A receptors that facilitates the relative saliency of rare auditory events over the frequent ones, as in the so-called *iceberg effect* [53]. The iceberg effect describes the observation whereby the spike output of a neuron under inhibition is more sharply tuned than the underlying membrane potential because only the strongest excitatory input sufficiently depolarizes the membrane to reach threshold for spike generation [32]. Thus, the enhancement of GABA_A-mediated inhibition increases SSA level [20]. On the other hand, propofol affects not only the IC but other brainstem structures as well. For example, pedunculo-pontine tegmental, nucleus and the lateral dorsal tegmental nucleus, the locus ceruleus, the dorsal raphe nucleus and ventral periaqueductal grey substance [9]. These brainstem arousal centers were silent during anesthesia but their electrical activity could stifle the IC

activity in clear consciousness.

Nevertheless, there is a possibility that the rare tone unique peak occurs for other reasons not related to deviance detection.

Cortex-brainstem interaction

The predominant number of Granger connections from brainstem to cortex in rare tone ERP on the time interval of rare tone unique peak (256-364 ms) points to midbrain-(frontal and central) cortex axis conductivity of brain tissues during deep anesthesia. There were no connections from brainstem to cortex in 600 Hz of equiprobability paradigm ERP and in noise ERP on the same time interval because there no prominent peak. The equal amount of cortex-to-cortex connections in two experimental paradigms and in noise ERP indicates the presence of similar minimal activity of the cortex, which serves to survival, in these three cases. The noise ERP connections wererandom.

In clear consciousness in rare tone ERP the majority of cortex-to-cortex connections was from frontal sites to other scalp sites. Such a distribution of cortex-to-cortex connections on the time interval of P300 (200-400 ms) reflects stimulus-driven frontal attention mechanisms during task processing [57]. The midbrain had only one connection: from lower to upper electrode, which shows possible conducting background auditory information from the IC to the cortex. Lower number of cortex-to-cortex connections in noise ERP comparing with experimental ERPs shows activation of the cortex in response to all types of sounds.

Conclusion

The data obtained suppose that:

1. The propofol affects the electrical activity of both human midbrain and cortex but the level of inhibition of the cortex by 6 times higher than the level of inhibition of the midbrain.
2. Human midbrain participates in mismatch detection and can do it even without the cognitive activity of cerebral cortex.

Acknowledgment

The study has been supported by RAS and RFFI № 18-013-00967a. Authors' contribution: project authorship, idea presentation and neurosurgical operation: DIP; conceived and designed the experiment: DIP, LBO, VVP; performed the experiment: DIP, LBO, VVP, OSZ, analyzed the data: LBO, AOK, ELM, wrote the paper: LBO, ELM, AOK, DIP, VVP.

Author Disclosure Statement

No competing financial interests exist.

References

1. Amzica F. Basic physiology of burst-suppression. *Epilepsia* 50 (2009): 38–39.
2. Andersen P, Andersson SA, Lomo T. Nature of thalamo-cortical relations during spontaneous barbiturate spindle activity. *The Journal of Physiology* 192 (1967): 283–307.

3. Ayala YA, Udeh A, Dutta K, Bishop D, Malmierca MS, Oliver DL. Differences in the strength of cortical and brainstem inputs to SSA and non-SSA neurons in the inferior colliculus. *Scientific Reports* 5 (2015).
4. Bai D, Pennefather PS, MacDonald JF, Orser BA. The general anesthetic propofol slows deactivation and desensitization of GABA (A) receptors. *J Neurosci* 19 (1999):10635–10646.
5. Bento RF, Neto RVB, Tsuji RK, Gomes MQT, Goffi-Gomez MVS. Auditory Brainstem Implant: surgical technique and early audiological results in patients with neurofibromatosis type 2. *Brazilian Journal of Otorhinolaryngology* 74 (2008): 647–651.
6. Biacabe B, Chevallier JM, Avan P, Bonfils P. Functional anatomy of auditory brainstem nuclei: application to the anatomical basis of brainstem auditory evoked potentials. *Auris Nasus Larynx* 28(2001): 85–94.
7. Bibikov NG. ‘Novelty’ neurons in the frog auditory system. *Zh. Vyssh. Nerv. Deiat. Im. I. P. Pavlova* 27 (1977): 1075–1082.
8. Brackmann DE, Hitselberger WE, Nelson RA, Moore J, Waring MD, Portillo F, et al. Auditory brainstem implant: I. Issues in surgical implantation. *Otolaryngol Head Neck Surg* 108 (1993): 624-33.
9. Brown EN, Purdon PL, Van Dort CJ. General Anesthesia and Altered States of Arousal: A Systems Neuroscience Analysis. *Annual Review of Neuroscience* 34 (2011):601–628.
10. Bulkin D and Groh J. Systematic mapping of the monkey inferior colliculus reveals enhanced low frequency sound representation. *J Neurophysiol* 105 (2011):1785–1797.
11. Cacciaglia R, Escera C, Slabu L, Grimm S, Sanjuán A, Ventura-Campos N, Ávila C. Involvement of the human midbrain and thalamus in auditory deviance detection. *Neuropsychologia* 68 (2015): 51–58.
12. Carbajal GV, Malmierca MS. The Neuronal Basis of Predictive Coding Along the Auditory Pathway: From the Subcortical Roots to Cortical Deviance Detection. *Trends in Hearing* 22 (2018): 233121651878482.
13. Chassard D, Colson A, Banskillon V, Joubaud A, Dubreuil C, Guiraud M. Auditory evoked potentials during propofol anaesthesia in man. *British Journal of Anaesthesia* 62 (1989): 522–526.
14. Chen YQ, Li NL, Liu H, Hu JQ, Wang DZ. Clinical study on applying brainstem auditory evoked potential to monitor anesthesia depth and awake in children. *Zhonghua Er Bi Yan Hou Ke Za Zhi* 38 (2003):118-20.
15. Ching S, Purdon PL, Vijayan S, Kopell NJ, Brown EN. A neurophysiological-metabolic model for burst suppression. *Proc Natl Acad Sci U S A* 109 (2012):3095–100.
16. Colletti V, Shannon R, Carner M, Veronese S, Colletti L. Outcomes in Nontumor Adults Fitted With the Auditory Brainstem Implant: 10 Years’ Experience. *Otol Neurotol* 30 (2009): 614-618.
17. Csepe V. On the origin and development of the mismatch negativity. *Ear and Hearing* 16 (1995): 91–104.
18. Donchin E, Coles MGH. Is the P300 component a manifestation of context updating? *Behav Brain Sci* 11 (1988): 357–427.
19. Duque D, Ayala YA, Malmierca MS. Deviance detection in auditory subcortical structures: what can we learn from neurochemistry and neural connectivity? *Cell and Tissue Research* 361 (2015): 215–232.
20. Duque D, Malmierca MS, Caspary DM. Modulation of stimulus-specific adaptation by GABAA receptor activation or blockade in the medial geniculate body of the anaesthetized rat. *Journal of Physiology* 592 (2014): 729–743.

21. Duque D, Wang X, Nieto-Diego J, Krumbholz K, Malmierca MS. Neurons in the inferior colliculus of the rat show stimulus-specific adaptation for frequency, but not for intensity. *Scientific Reports* 6 (2016).
22. Engel AK, Fries P. Beta-band oscillations—signalling the status quo? *Current Opinion in Neurobiology* 20 (2010): 156–165.
23. Fernandes NF, Goffi-Gomez MVS, Magalhães ATDM, Tsuji RK, De Brito RV, Bento RF. Satisfação e qualidade de vida em usuários de implante auditivo de tronco cerebral. *CoDAS* 29 (2017).
24. Fernández-Bouzas A, Harmony T, Marosi E, Fernández T, Silva J, Rodríguez M, Bernal J, Reyes A, Casián G. Evolution of cerebral edema and its relationship with power in the theta band. *Electroencephalogr Clin Neurophysiol* 102 (1997):279-85.
25. Fiset P, Paus T, Daloz T, Plourde G, Meuret P, Bonhomme V, Hajj-Ali N, Backman SB, Evans AC. Brain mechanisms of propofol-induced loss of consciousness in humans: a positron emission tomographic study. *J Neurosci* 19 (1999):5506-5513.
26. Glasberg BR, Moore BCJ. Prediction of absolute thresholds and equal-loudness contours using a modified loudness model. *The Journal of the Acoustical Society of America* 120 (2006): 585–588.
27. Goffi-Gomez MVS, Magalhães AT, Brito R No, Tsuji RK, Gomes MDQT, Bento RF. Auditory brainstem implant outcomes and MAP parameters: report of experiences in adults and children. *Int J Pediatr Otorhinolaryngol* 76 (2012):257-64.
28. Grimm S, Escera C, Slabu L, Costa-Faidella J. Electrophysiological evidence for the hierarchical organization of auditory change detection in the human brain. *Psychophysiology* 48 (2011): 377–384.
29. Hemmings HC, Jr, Akabas MH, Goldstein PA, Trudell JR, Orser BA, Harrison NL. Emerging molecular mechanisms of general anesthetic action. *Trends Pharmacol Sci.* 26 (2005): 503–510.
30. Holsheimer J, Boer J, Lopes Da Silva FH, van Rotterdam A. The double dipole model of theta rhythm generation: Simulation of laminar field potential profiles in dorsal hippocampus of the rat. *Brain Research* 235 (1982): 31–50.
31. Holt F, Özdamar Ö. Effects of rate (0.3–40/s) on simultaneously recorded auditory brainstem, middle and late responses using deconvolution. *Clinical Neurophysiology* 127 (2016): 1589–1602.
32. Isaacson JS, Scanziani M. How inhibition shapes cortical activity. *Neuron* 72 (2011): 231–243.
33. Kaisti KK, Metsähonkala L, Teräs M, Oikonen V, Aalto S, Jääskeläinen S, Hinkka S, Scheinin H. Effects of Surgical Levels of Propofol and Sevoflurane Anesthesia on Cerebral Blood Flow in Healthy Subjects Studied with Positron Emission Tomography. *Anesthesiology* 96 (2002):1358–70.
34. Komune N, Yagmurlu K, Matsuo S, Miki K, Abe H, Rhoton AL. Auditory Brainstem Implantation. *Neurosurgery* 11 (2015): 306–321.
35. Lee MG, Chrobak JJ, Sik A, Wiley RG, Buzsáki G. Hippocampal theta activity following selective lesion of the septal cholinergic system. *Neuroscience* 62 (1994):1033–1047.
36. Leung LW. Model of gradual phase shift of theta rhythm in the rat. *Journal of Neurophysiology* 52 (1984): 1051–1065.
37. Lopes Da Silva FH, Storm Van Leeuwen W. The cortical source of the alpha rhythm. *Neuroscience Letters* 6 (1977): 237–241.

38. Lopes da Silva FH. Hippocampal RSA in humans. *Trends in Neurosciences* 14 (1991): 138.
39. Malerbi AF dos S, Goffi-Gomez MVS, Tsuji RK, Gomes M de QT, Brito Neto R de, Bento RF. Auditory brainstem implant in postmeningitis totally ossified cochleae. *Acta Oto-Laryngologica* 138 (2018): 722–726.
40. Malmierca MS, Cristaudo S, Perez-Gonzalez D, Covey E. Stimulus-Specific Adaptation in the Inferior Colliculus of the Anesthetized Rat. *Journal of Neuroscience* 29 (2009): 5483–5493.
41. Miller R, Eriksson L, Fleisher L, Wiener J et al. *Miller's Anesthesia, 2-Volume Set 8th Edition* (2014).
42. Moore BCJ, Glasberg BR, Baer T. A model for the prediction of thresholds, loudness and partial loudness. *J Audio Eng Soc* 45 (1997): 224–240.
43. Moore RY, Bloom FE. Central catecholamine neuron systems: anatomy and physiology of the norepinephrine and epinephrine systems. *Annual Review of Neuroscience* 2 (1979): 113-168.
44. Muller CM, Lewandowski MH, Singer W. Structures mediating cholinergic reticular facilitation of cortical responses in the cat: effects of lesions in immunocytochemically characterized projections. *Experimental Brain Research* 96 (1993): 8-18.
45. Naatanen R, Picton T. The N1 wave of the human electric and magnetic response to sound: a review and an analysis of the component structure. *Psychophysiology* 24 (1987): 375–425.
46. Nakatomi H, Miyawaki S, Kin T, Saito N. Hearing Restoration with Auditory Brainstem Implant. *Neurologia Medico-Chirurgica* 56 (2016): 597–604.
47. Oknina LB, Kantserova AO, Masherov EL, Podlepich VV, Zaitsev OS, Pitskhelauri DI. Functional connectivity between the midbrain and cortex during consciousness recovery after general anesthesia. *Wjpmr* 5 (2019): 237-249.
48. Otto SR, Brackmann DE, Hitselberger WE, Shannon RV, Kuchta J. Multichannel auditory brainstem implant: update on performance in 61 patients. *J Neurosurg* 96 (2002): 1063-71.
49. Pare D, Smith Y, Parent A, Steriade M. Projections of brainstem core cholinergic and noncholinergic neurons of cat to intralaminar and reticular thalamic nuclei. *Neuroscience* 25 (1988): 69-86.
50. Parsons CE, Young KS, Joensson M, Brattico E, Hyam JA, Stein A, Kringelbach ML. Ready for action: a role for the human midbrain in responding to infant vocalizations. *Social Cognitive and Affective Neuroscience* 9 (2013): 977–984.
51. Parvizi J, Damasio A. Consciousness and the brainstem. *Cognition*. 79 (2001):135-60.
52. Patel CR, Redhead C, Cervi AL, Zhang H. Neural sensitivity to novel sounds in the rat's dorsal cortex of the inferior colliculus as revealed by evoked local field potentials. *Hearing Research* 286 (2012): 41–54.
53. Pérez-González D, Hernández O, Covey E, Malmierca MS. GABAA-mediated inhibition modulates stimulus-specific adaptation in the inferior colliculus. *PLoS One* 7 (2012): e34297.
54. Pérez-González D, Malmierca MS, Covey E. Novelty detector neurons in the mammalian auditory midbrain. *European Journal of Neuroscience* 22(2005): 2879–2885.
55. Picton TW, Hillyard SA, Krausz HI, Galambos R. Human auditory evoked potentials. I: Evaluation of components. *Electroencephalography and Clinical Neurophysiology* 36 (1974): 179-190.

56. Pitskhelauri DI, Konovalov AN, Kornienko VN, Serova NK, Arutiunov NV, Kopachev DN. Intraoperative direct third ventriculostomy and aqueductal stenting in deep-seated midline brain tumors surgery. *Neurosurgery* 64 (2009): 256-267.
57. Polich J. Updating P300: an integrative theory of P3a and P3b. *Clin Neurophysiol* 118 (2007): 2128–2148.
58. Purdie JAM, Cullen PM. Brainstem auditory evoked response during propofol anaesthesia in children. *Anaesthesia* 48 (1993): 192–195.
59. Purdon PL, Sampson A, Pavone KJ, Brown EN. Clinical Electroencephalography for Anesthesiologists. *Anesthesiology* 123 (2015): 937–960.
60. Rampil I. Consciousness, awareness, and the clinician. *Can J Anesth* 50 (2003): R1–R5.
61. Rampil IJ, Weiskopf RB, Brown JG, Eger EI, 2nd, Johnson BH, Holmes MA, Donegan JH. I653 and isoflurane produce similar dose-related changes in the electroencephalogram of pigs. *Anesthesiology* 69 (1988): 298–302.
62. Robinson BL, Harper NS, McAlpine D. Meta-adaptation in the auditory midbrain under cortical influence. *Nat Commun* 7 (2016): 13442.
63. Schwartz MS, Wilkinson EP. Auditory brainstem implant program development. *The Laryngoscope* 127 (2016): 1909–1915.
64. Schwender D, Madler C, Klasing S, Pöppel E, Peter K. Monitoring intraoperative processing of acoustic stimuli with auditory evoked potentials. *Infusionsther Transfusionsmed* 5 (1993): 272-6.
65. Skoe E, Chandrasekaran B, Spitzer ER, Wong PCM, Kraus N. Human brainstem plasticity: The interaction of stimulus probability and auditory learning. *Neurobiology of Learning and Memory* 109 (2014): 82–93.
66. Slabu L, Grimm S, Escera C. Novelty detection in the human auditory brainstem. *Journal of Neuroscience* 25 January 32 (2012): 1447-1452.
67. Steriade M. Central core modulation of spontaneous oscillations and sensory transmission in thalamocortical systems. *Current Opinion in Neurobiology* 3 (1993): 619-625.
68. Stewart M, Fox SE. Do septal neurons pace the hippocampal theta rhythm? *Trends in Neurosciences* 13 (1990): 163–169.
69. Vasudeva RK, Lin RCS, Simpson KL, Waterhouse BD. Functional organization of the dorsal raphe efferent system with special consideration of nitrenergic cell groups. *Journal of Chemical Neuroanatomy* 41 (2011): 281–293.
70. Verleger R. On the utility of P3 latency as an index of mental chronometry. *Psychophysiology* 34 (1997): 131–156.
71. Wong K, Kiringoda R, Kanumuri VV, Barber SR, Franck K, Sahani N, Brown MC, Herrmann BS, Lee DJ. Effect of anesthesia on evoked auditory responses in pediatric auditory brainstem implant surgery. *Laryngoscope* (2019).

Citation: Anna O. Kantserova, Lyubov B. Oknina, Eugeny L. Masherov, Vitaly V. Podlepich, Oleg S. Zaitsev and David I. Pitskhelauri. Human Midbrain Participates In Mismatch Detection Without Cognitive Activity Of The Cerebral Cortex: Case Report. Archives of Clinical and Biomedical Research 3 (2019): 296-314.



This article is an open access article distributed under the terms and conditions of the [Creative Commons Attribution \(CC-BY\) license 4.0](https://creativecommons.org/licenses/by/4.0/)